International Journal of Engineering Trends and Technology
ISSN: 2231–5381 / https://doi.org/10.14445/22315381/IJETT-V74I1P108

Volume 74 Issue 1, 108-116, January 2026

Original Article

Performance Analysis of Virtual Synchronous Machine-Based 13-Level Cascaded H-Bridge Statcom

K. Varalakshmi[1], R. L. Narsimham[2], G. Tulasi Ramdas[3]

[1]*Department of Electrical and Electronics, Aditya University, Andhra Pradesh, India.*
[2]*Department of Electrical and Electronics, Andhra University, Andhra Pradesh.*
[3]*Department of Electrical and Electronics, JNTU-Hyderabad, Telangana.*

[1]*Corresponding Author : vara1981@gmail.com*

Received: 22 May 2025 Revised: 19 December 2025 Accepted: 25 December 2025 Published: 14 January 2026

Abstract *- For adjustable reactive power compensation in the distribution system, a STATCOM is interconnected between the primary source and load. The design of the STATCOM defines the quality of the reactive power compensation on the grid. In this paper, a virtual synchronous machine-based 13-level cascaded H-bridge STATCOM is proposed. The 13-level cascaded H-bridge structure of the STATCOM reduces harmonics in the grid voltage and current. As the STATCOM is a static reactive power compensation device, the inertia of the circuit is very low, which creates peak voltages and currents in the grid. To make the STATCOM operate as a dynamic machine, a VSM concept is introduced in the controller. The VSM-based controller is included with inertia control, which makes the STATCOM work as an overexcited asynchronous machine. With inertia introduced in the control, the peak overshoots in the voltages and currents are reduced, stabilizing the system. The VSM control generates reference signals for the 13-level cascaded H-bridge STATCOM, taking feedback from the PCC voltages and collective DC link voltages of the H-bridges. The reference signals' magnitude and phase are controlled as per the demand on the grid side. The modeling and design of the proposed system is carried out in MATLAB Simulink software, with results analyzed as per different operating conditions.*

Keywords *- Static Synchronous Compensator, 13-level Cascaded H-bridge, Virtual Synchronous Machine (VSM), Point of Common Coupling (PCC), MATLAB Simulink.*

1. Introduction

In modern power systems, the power demand is increasing day by day as the number of consumers on the grid increases. The power demand by these consumers in commercial and industrial sectors has drastically increased as the production and supply demand chain is expanding. In the manufacturing sector, the reactive power demand is very high as the machinery used as a load consumes high reactive power. The increased demand for reactive power from the grid creates power quality issues like voltage sag, harmonics, fluctuations, etc. The power factor of the source also drops as the reactive power demanded by the load needs to be compensated by the source itself [1].

To avoid these issues of power quality and disturbances in the grid, reactive power compensation devices need to be interconnected between the source and the load [2]. The conventional methods to compensate reactive power are by connecting an overexcited asynchronous machine or static capacitor banks. However, these methods have no specific control over the injection of reactive power to the grid, which may lead to overcompensation, creating a swell in the voltages [3]. Voltage swells are considered to be more fatal than voltage sags, as the equipment connected to the line with overcompensation may damage the circuits with the overvoltage. Therefore, these modules are replaced with a Flexible AC Transmission (FACT) device, STATCOM, which compensates the reactive power as per the requirement of the load [4].

By keeping the compensation within a limit as per the load demand, voltage occurrence can be completely avoided. The equipment connected to the system with STATCOM devices is also protected with no overcompensation issues. The STATCOM is a static device that comprises power electronic switches and a capacitor bank [4].

The controller of the STATCOM takes feedback from the source voltages and load currents for the reactive power compensation. The STATCOM device is operated in synchronization with the grid voltage since it is connected in shunt to the grid at the PCC. A typical outline diagram of a STATCOM device connected to the grid with reactive power load demand can be observed in Figure 1.

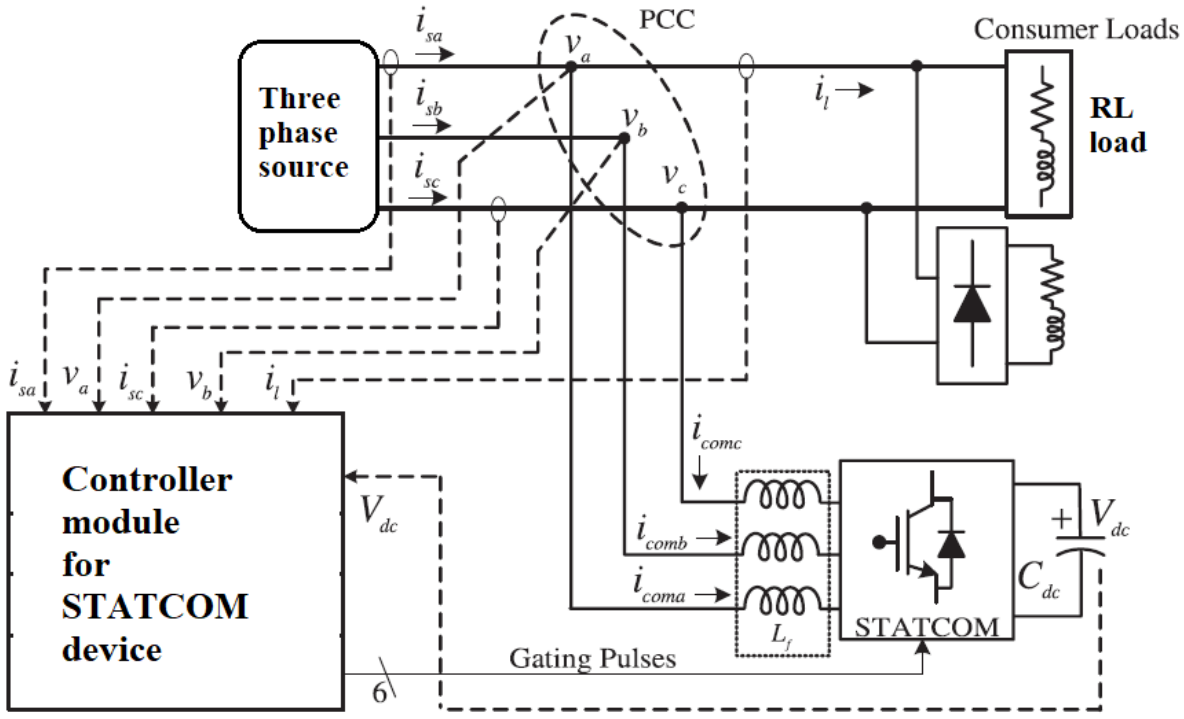

Fig. 1 Structure of the STATCOM-connected system

As per the presented Figure 1, all the modules (three-phase source, RL load, and STATCOM) are connected at The PCC, where the powers are shared and compensated. The RL load connected needs both active and reactive powers for compensation. Reactive power consumption from the grid increases power loss and reduces the power factor of the source, creating voltage sags [5]. The reactive power is compensated by the 13-level cascaded H-bridge STATCOM with VSM capability [6]. The VSM controller is included with virtual inertia and virtual impedance, which makes the STATCOM operate as a controlled dynamic synchronous condenser. The virtual inertia considers two components, D and M, which are the virtual damping coefficient and virtual angular momentum. The virtual impedance also has two components, L and R, which are the inductance and resistance of the filter L_f connected between the STATCOM and PCC [7].

1.1. Limitations and Future Scope

Previous studies have primarily implemented VSM control through droop mechanisms for inverter-based DG. The droop controller features active- and reactive-power loops that generate magnitude and phase-angle reference signals, where magnitude governs reactive power compensation and phase regulates active power exchange. To emulate synchronous generator behaviour, droop-based DG controllers are further enhanced with virtual inertia and virtual impedance. Following the same principle, in this work, the reactive-power control loop of the STATCOM incorporates virtual inertia and virtual impedance to replicate the dynamics of an over-excited synchronous machine, thereby improving stability during transients.

The VSM–STATCOM module is primarily suitable for integration in distribution networks and is generally not recommended for transmission-level applications. The control parameter tuning in the VSM architecture is highly complex, and its dynamic response can be relatively slow during rapid system disturbances. Moreover, under weak-grid conditions, the operational performance of the VSM deteriorates, reducing its overall effectiveness in maintaining system stability.

Additionally, the requirement for sophisticated control hardware and advanced software increases the overall cost of the module. Future advancements may include replacing conventional PI controllers with adaptive or hybrid regulation techniques to achieve faster dynamic response and improved settling times. Upgrading the existing modulation strategy to Space Vector Modulation (SVM) can further help in reducing harmonic distortion and enhancing power quality.

This paper is organized with Section 1 including an introduction to the proposed system, followed by the configuration of a 13-level cascaded H-bridge STATCOM. The design of the VSM control for the STATCOM is presented in Section 3 with complete structure details of the controller. The results of the analysis and comparison of the proposed model with the conventional STATCOM model are presented in Section 4. The validation of the optimal operation

of the VSM-STATCOM is determined by the result analysis. The final section 5 is the conclusion to the paper, finalizing the obtained results from the designed model and discussing the advantages of the proposed system, followed by references cited in the paper.

2. Cascaded H-bridge 13-level STATCOM Configuration

Multi-level converters are an advancement to conventional two-level Voltage Source Converters (VSC), which have heavy harmonic content. The increased number of voltage levels replicates a Sinusoidal wave, reducing the harmonic content of the voltages and currents. There are many types of multi-level converters, which include diode clamp, switched capacitor, etc. The most basic, less complex, and robust multi-level converter is a cascaded H-bridge multilevel converter [8]. For increasing the levels of the converter, the number of H-bridges needs to be increased. The Number Of Levels (M) is determined as per the number of H-bridges (N) connected in the circuit, which is given as [9]:

$$M = 2 * N + 1 \quad (1)$$

Therefore, for 13-level voltages, 6 H-bridges are connected in series for each phase of the circuit. Each H-bridge comprises four IGBT switches (S1-S4), with diagonal switches operating simultaneously [10]. The circuit structure of the 13-level cascaded H-bridge converter of one phase with DC link capacitors operated as STATCOM is presented in Figure 2. All 6 H-bridges are included with a capacitor on the DC side of charging from the grid, consuming leading current. The leading current consumption from the grid injects reactive power, which is consumed by the heavy RL load connected to the grid. This improves the power factor of the source, and the voltage sag created by the RL load is mitigated, improving the voltage profile of the system [11]. The Figure 2 circuit structure is used for the other two phases, also creating a phase 13-level cascaded H-bridge converter STATCOM.

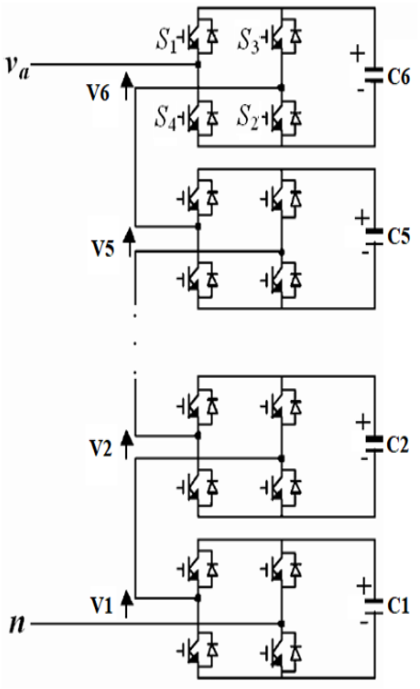

Fig. 2 13-level cascaded H-bridge converter

The IGBT switches of the converter are controlled by the Phase Disposition Pulse Width Modulation (PD-PWM) technique. The PD-PWM technique compares a reference Sinusoidal waveform to multiple level-shifted high-frequency triangular waveforms, creating pulses to the IGBTs [12]. The PD-PWM technique with reference modulation and carrier signals is presented in Figure 3. In the given Figure 3, the u_1–u_6 are the carrier signals, and u_{ref} is the reference modulation signal, which is generated by the VSM controller. For the generation of pulses to 6 H-bridges for 13-level voltages, each region (positive and negative) has 6 triangular carrier signals generating pulses for 24 switches of one phase [13]. The switching states of each switch of one phase of the 13-level cascaded H-bridge are given in Table 1.

Table 1. 13-level cascaded H-bridge converter switching states

Voltage level	Switching states																							
	S_1	S_2	S_3	S_4	S_5	S_6	S_7	S_8	S_9	S_{10}	S_{11}	S_{12}	S_{13}	S_{14}	S_{15}	S_{16}	S_{17}	S_{18}	S_{19}	S_{20}	S_{21}	S_{22}	S_{23}	S_{24}
0	0	1	0	1	0	1	0	1	0	1	0	1	0	1	0	1	0	1	0	1	0	1	0	1
Vdc/6	1	1	0	0	0	0	0	0	0	0	0	0	0	0	0	0	0	0	0	0	0	0	0	0
2Vdc/6	1	1	0	0	1	1	0	0	0	0	0	0	0	0	0	0	0	0	0	0	0	0	0	0
3Vdc/6	1	1	0	0	1	1	0	0	1	1	0	0	0	0	0	0	0	0	0	0	0	0	0	0
4Vdc/6	1	1	0	0	1	1	0	0	1	1	0	0	1	1	0	0	0	0	0	0	0	0	0	0
5Vdc/6	1	1	0	0	1	1	0	0	1	1	0	0	1	1	0	0	1	1	0	0	0	0	0	0
Vdc	1	1	0	0	1	1	0	0	1	1	0	0	1	1	0	0	1	1	0	0	1	1	0	0
-Vdc/6	0	0	1	1	0	0	0	0	0	0	0	0	0	0	0	0	0	0	0	0	0	0	0	0
-2Vdc/6	0	0	1	1	0	0	1	1	0	0	0	0	0	0	0	0	0	0	0	0	0	0	0	0
-3Vdc/6	0	0	1	1	0	0	1	1	0	0	1	1	0	0	0	0	0	0	0	0	0	0	0	0
-4Vdc/6	0	0	1	1	0	0	1	1	0	0	1	1	0	0	1	1	0	0	0	0	0	0	0	0
-5Vdc/6	0	0	1	1	0	0	1	1	0	0	1	1	0	0	1	1	0	0	1	1	0	0	0	0
-Vdc	0	0	1	1	0	0	1	1	0	0	1	1	0	0	1	1	0	0	1	1	0	0	1	1

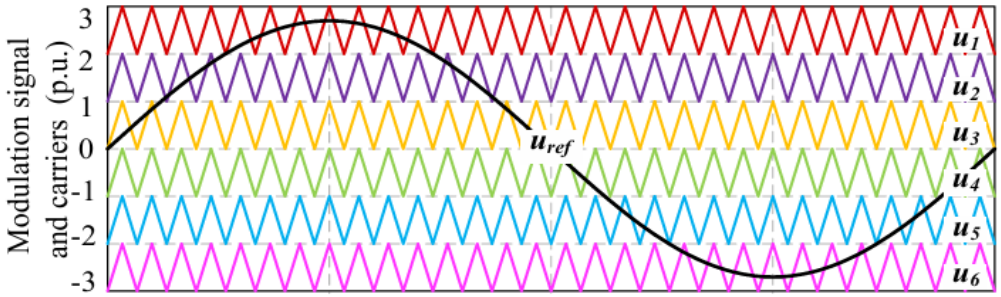

Fig. 3 PD-PWM technique comparison signals

3. VSM Controller Design

As the STATCOM is a static device with power electronic switches and capacitive elements, there is zero inertia in the device. As compared to an overexcited synchronous machine, which is dynamic in nature, it has high inertia [14]. This reduces the disturbances in the compensator for any sudden changes in the grid. Due to the inertia, the peak overshoots, and high damping is reduced. As the STATCOM device cannot be changed to a dynamic state, the controller that generates the reference Sinusoidal signals is introduced with virtual inertia. With this update, the basic STATCOM is converted to VSM-STATCOM with virtual inertia inclusion [15]. The proposed structure of VSM control with virtual inertia and virtual impedance is presented in Figure 4.

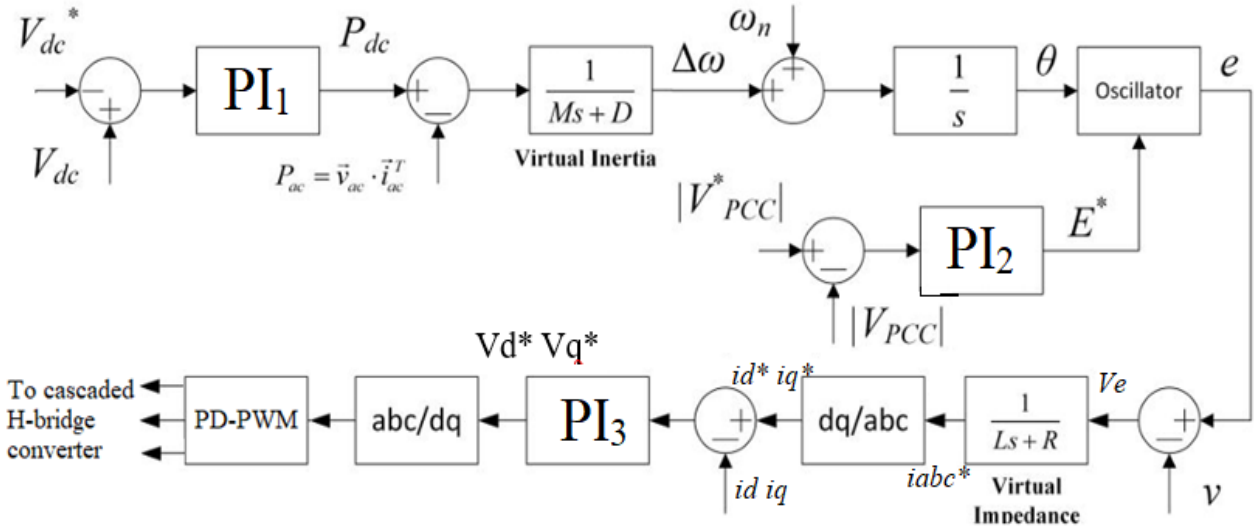

Fig. 4 VSM control structure

The VSM control structure needs measurements of accumulated DC link voltage of the STATCOM capacitors (V_{dc}), active power of the grid source (P_{ac}), grid fundamental angular frequency (w_n), PCC voltage (V_{PCC}), STATCOM voltage (v), and current (i) [16]. The final Vd* Vq* components for the inverse Park's transformation are generated by the PI current regulator by the expressions given as:

$$V_d^* = (i_d^* - i_d)\left(K_{p3} + \frac{K_{i3}}{s}\right) \quad (2)$$

$$V_q^* = (i_q^* - i_q)\left(K_{p3} + \frac{K_{i3}}{s}\right) \quad (3)$$

Here, i_d i_q are the measured STATCOM dq components generated by the Park's transformation of STATCOM currents (I_{abc}), and i_d* and i_q* are generated by the 'virtual impedance' and error voltage (V_e) component given as [17]:

$$i_d^* = (v - e)\left(\frac{1}{Ls+R}\right) \quad (4)$$

Here, v is the STATCOM voltages (Vabc), L and R are the inductance and resistance of the filter connected between STATCOM and PCC, respectively. e is the corrected voltage component generated, given as:

$$e = E^*.Sin\,\theta \quad (5)$$

The E^* Is the magnitude of the correct voltage, and θ is the phase angle of phase A. The other two phases, correction signals (e_b e_c), are generated with a phase shift of -120 and +120 degrees. The magnitude E^* is calculated as [18]:

$$E^* = (V^*_{PCC} - V_{PCC})\left(K_{p2} + \frac{K_{i2}}{s}\right) \quad (6)$$

Herem V^*_{PCC} Is the reference PCC voltage magnitude set as '1' as the controller is structured in perunit. The phase angle θ is generated from the change in frequency ($\Delta\omega$) signal and w_n expressed as:

$$\theta = \frac{w_n + \Delta\omega}{s} \quad (7)$$

The change in frequency ($\Delta\omega$) is calculated by the virtual inertia and active powers comparison given as:

$$\Delta\omega = (P_{dc} - P_{ac})\left(\frac{1}{Ms+D}\right) \quad (8)$$

Here, D and M are the virtual damping coefficient and virtual angular momentum, P_{ac} is the source active power, and DC active power (P_{dc}) is given as:

$$P_{dc} = (V^*_{dc} - V_{dc})\left(K_{p1} + \frac{K_{i1}}{s}\right) \quad (9)$$

From these expressions, including virtual inertia and virtual impedance, the final reference signals (Vabc*) are generated, which are compared to PD-PWM carrier waveforms, generating pulses to the 13-level cascaded multi-level converter [19]. The modeled control structure is updated to the model, and the simulation comparative analysis is done in the next section.

4. Results and Discussion

The modeling and analysis of the proposed system with simple PD-PWM control and VSM, including PD-PWM of the 13-level cascaded H-bridge STATCOM, is done. The simulation modeling is done using 'Electrical' blocks from the Simulink library browser of MATLAB software. All the electrical blocks are considered from 'Power electronics', 'Electrical sources', 'Measurements' of the 'Simpowersystems' subsets. The model is updated with the given configuration parameter, as shown in Table 2.

Table 2. Configuration parameters

Name of the module	Parameters
Grid	11kV, 50Hz, 10MVA
Load	Transformer: 0.5MVA 11kV/440V Load 1: 100kW 50kVAR Load 2: 5.5MVA, 3MVAR
STATCOM	R_{igbt} = 1mΩ, C_{dc} = 810μF, L_f = 10mH
VSM control	Vdc* = 11000*$\sqrt{2}$, Pac = 0, $w_n = 2\pi 50$, Vpcc* = 1, M = 0.01, D = 0.1/π

As per the given parameters, the simulations without and with VSM control are modelled. The simulation is run for 1.5s with different operating conditions created on the grid. To create a voltage sag, heavy Load 2 is connected to the grid at 0.2s, which consumes 3MVAR from the primary source. This reactive power needs to be compensated by the STATCOM device, which is connected at 0.4s, injecting reactive power at the PCC. The complete graphs of voltages and powers of the modules of the proposed model are presented with respect to time.

The given Figures 5 and 6 are the three-phase load voltages and currents varying as per the load and STATCOM connections. The load voltage magnitude drastically drops to 0.5pu when the heavy load 2 is connected at 0.2s, creating a voltage sag. And when the STATCOM device is connected at 0.4s, the voltage magnitudes gradually increase to 1pu until 0.55s. There is also a significant increase in the current magnitude as the STATCOM injects reactive power to the load, compensating for the required power. Figure 7 represents the DC link voltages of the capacitors connected on the DC side of the H-bridges of the cascaded circuit. Each capacitor has an increased voltage level as the voltage is divided between the H-bridges. The first DC link capacitor has the lowest voltage of 700V, and the last capacitor has the highest voltage of 3300V. As per the leading current consumption by the DC link capacitors, the active and reactive power exchange from the STATCOM is recorded and presented in Figure 8 graphs.

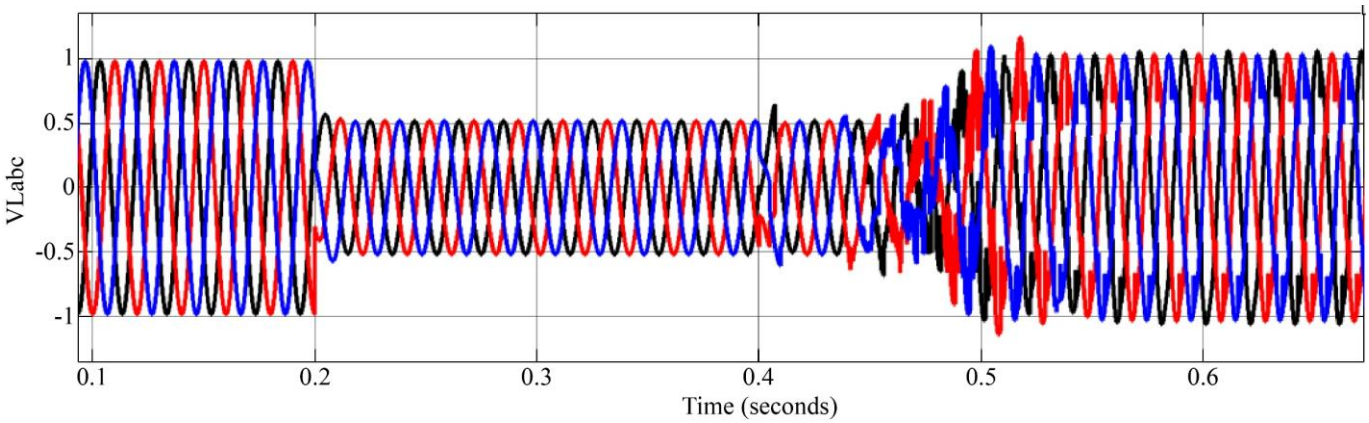

Fig. 5 Three-phase load voltages

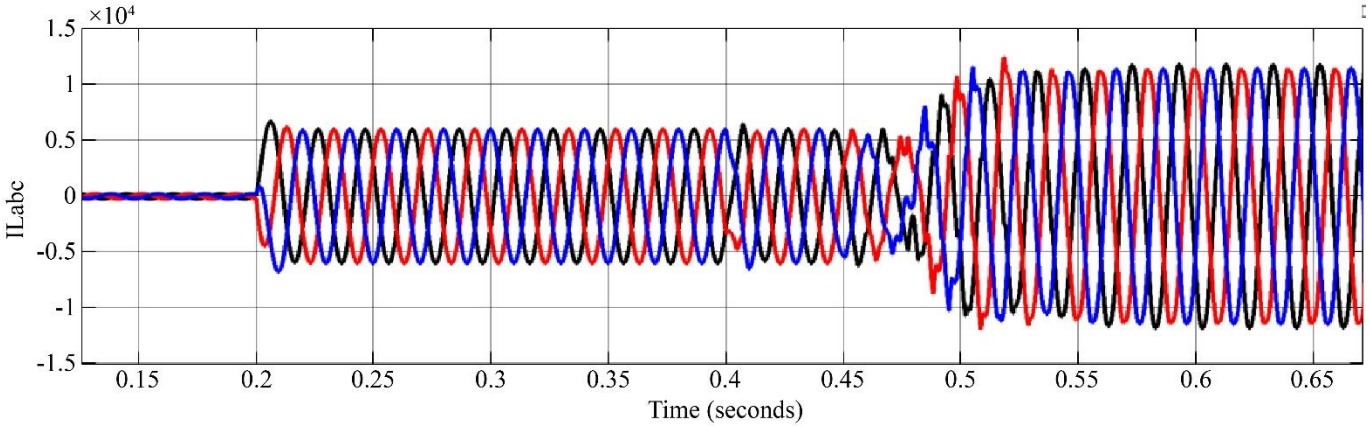

Fig. 6 Three three-phase load currents

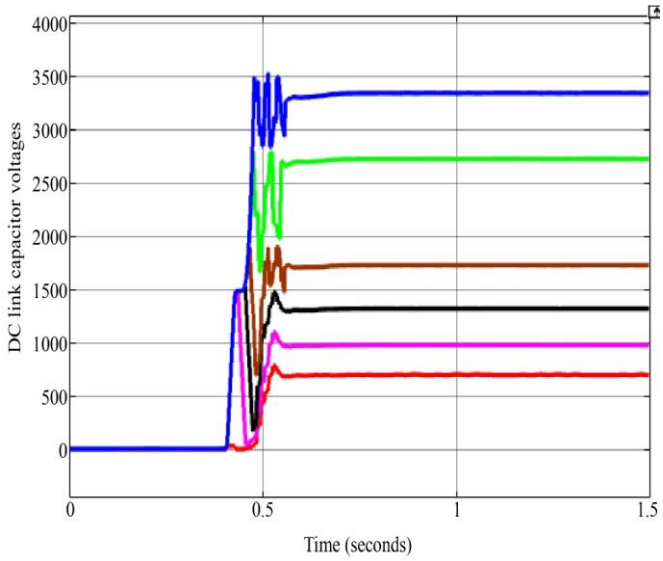

Fig. 7 DC link voltages of the H-bridge capacitors

As per Figure 8, there is a small active power consumption by the STATCOM in the range of 0.3MW, which is caused by the conduction of IGBT, filter resistance, and capacitors' resistance. A total reactive power of 35MVAR is injected into the grid, from which some part of the power is directed to load reactive power compensation. This increases the load voltage magnitude back to 1pu as the heavy load reactive power is compensated by the STATCOM.

Figure 9 represents the load voltage magnitude comparison of all three phases without and with VSM. As observed, the settling time of the load voltage magnitude of all the phases settles more slowly for the system with VSM included. However, the ripple in the magnitude is significantly lower for the VSM inclusive STATCOM model. This represents that the system is more stable with reduced disturbances and oscillations when the STATCOM is controlled by VSM control, including virtual inertia and virtual impedance.

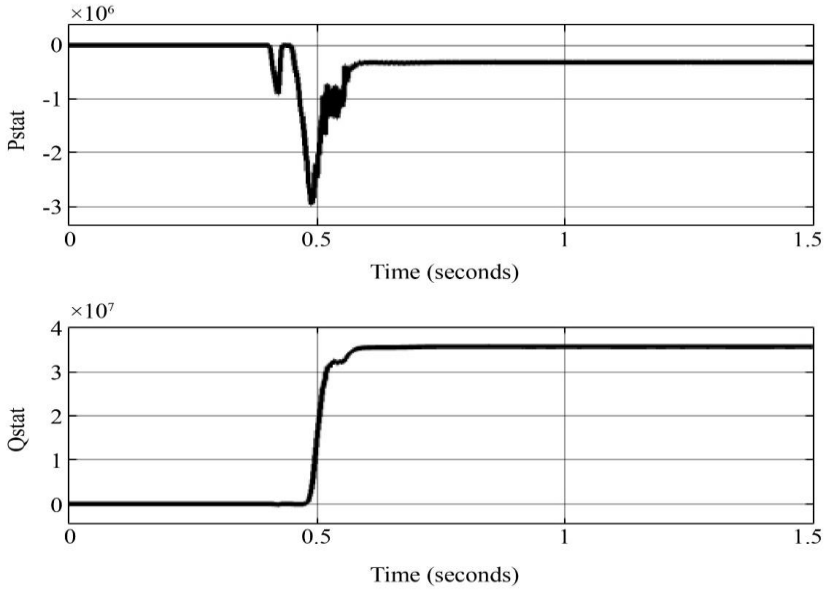

Fig. 8 Active and reactive powers of STATCOM

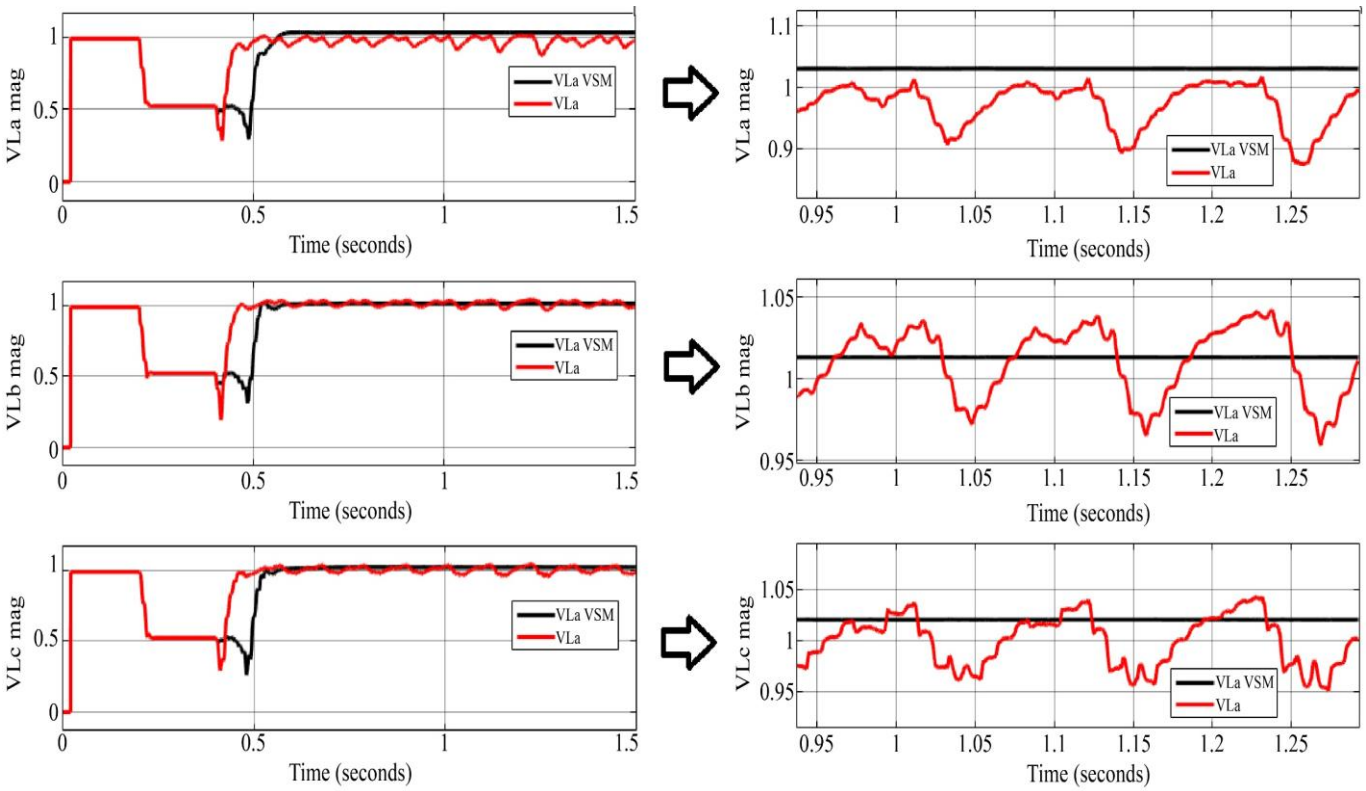

Fig. 9 Load voltage magnitudes comparison

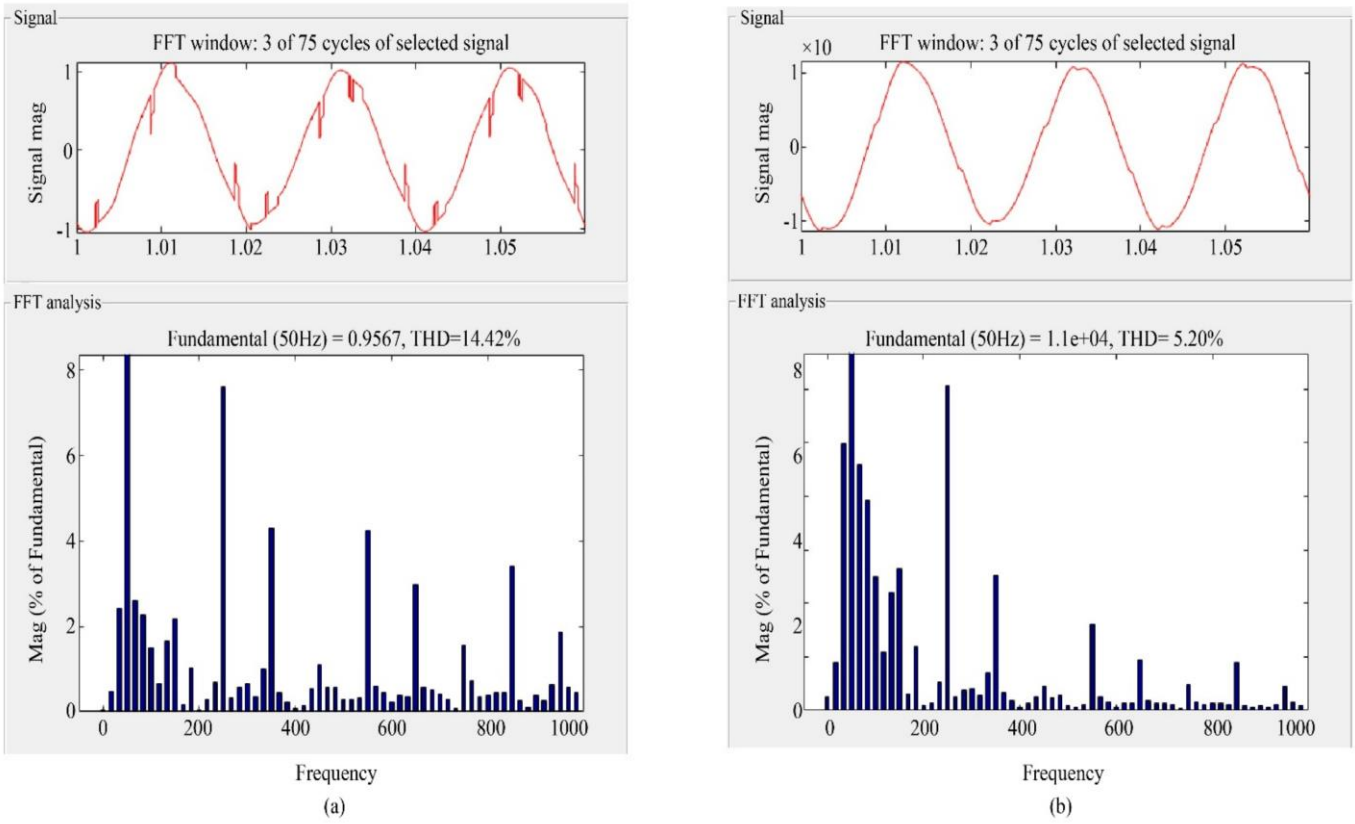

Fig. 10 THDs without VSM of (a) Load Voltage, and (b) Load current.

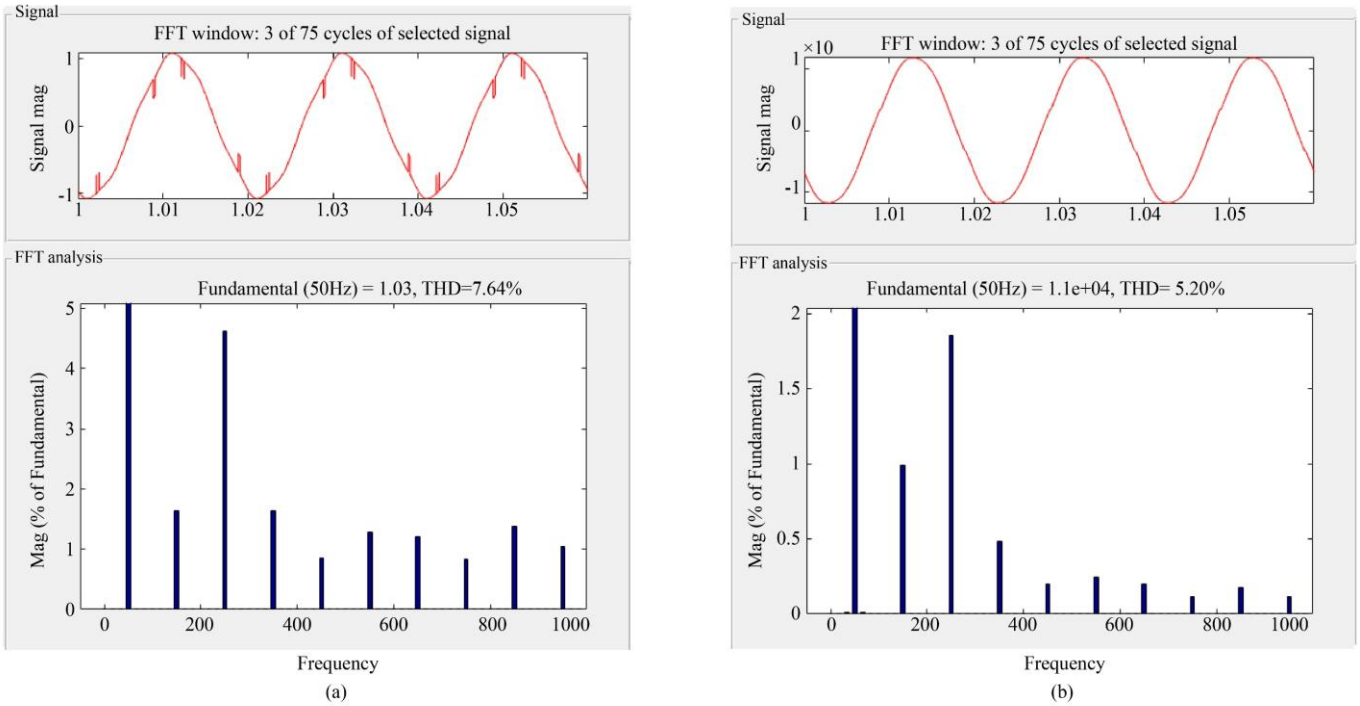

Fig. 11 THDs with VSM of (a) Load voltage, and (b) Load current.

As per the reduced disturbances in the reference signals V_{abc}*, the harmonics in the load voltage and current are also decreased to a greater extent. With the FFT analysis tool in Simulink 'powergui', the THDs of the load voltage and current are calculated and presented in Figures 10(a), 10(b), and 11(a), 11(b). Figures 10(a) and 10(b) are the load voltage and current THDs without VSM control. Figures 11(a) and 11(b) are the load voltage and current THDs with VSM control. A comparison Table 3 of different parameters of the proposed system without and with VSM control is presented below.

Table 3. Comparison table

Name of the parameter	Without VSM	With VSM
Vmag ripple	10.52%	1.2%
THD of VLoad	14.42%	7.64%
THD of ILoad	5.2%	2.22%

5. Conclusion

This paper presents the modeling and performance evaluation of a VSM-based STATCOM incorporating virtual inertia and virtual impedance. The proposed controller enables the inherently static STATCOM to emulate the behavior of a dynamic synchronous condenser, allowing reactive power injection with an inertia factor.

The 13-level cascaded H-bridge topology effectively reduces harmonic distortion due to its high number of voltage levels. However, in the absence of inertia, disturbances arise in the reference signals, resulting in voltage magnitude ripple and increased harmonic content in both voltage and current waveforms.

By integrating the VSM concept into the PD-PWM control scheme, virtual inertia significantly suppresses disturbances in the reference signal generation, thereby enhancing the overall performance of the 13-level cascaded H-bridge STATCOM. As a result, notable improvements are achieved, including a reduction in voltage magnitude ripple from 10.52% to 1.2%, and a decrease in total harmonic distortion from 14.42% to 7.64% in the load voltage and from 5.2% to 2.22% in the load current.

References

[1] Shazma Khan, Balvinder Singh, and Prachi Makhija, "A Review on Power Quality Problems and its Improvement Techniques," *2017 Innovations in Power and Advanced Computing Technologies (i-PACT)*, Vellore, India, pp. 1-7, 2017. [CrossRef] [Google Scholar] [Publisher Link]

[2] Manish Srivastava et al., "A Review on Power Quality Problems, Causes and Mitigation Techniques," *2022 1st International Conference on Sustainable Technology for Power and Energy Systems (STPES)*, Srinagar, India, pp. 1-6, 2022. [CrossRef] [Google Scholar] [Publisher Link]

[3] Mohammed Barghi Latran, Ahmet Teke, and Yeliz Yoldaş, "Mitigation of Power Quality Problems using Distribution Static Synchronous Compensator: A Comprehensive Review," *IET Power Electronics*, vol. 8, no. 7, pp. 1312-1328, 2015. [CrossRef] [Google Scholar] [Publisher Link]

[4] Kamel Djamel Eddine Kerrouche et al., "Modeling and Design of the Improved D-STATCOM Control for Power Distribution Grid," *SN Applied Sciences*, vol. 2, no. 9, pp. 1-11, 2020. [CrossRef] [Google Scholar] [Publisher Link]

[5] Sandeep Sharma et al., "A Comprehensive Review on STATCOM: Paradigm of Modeling, Control, Stability, Optimal Location, Integration, Application, and Installation," *IEEE Access*, vol. 12, pp. 2701-2729, 2024. [CrossRef] [Google Scholar] [Publisher Link]

[6] Chi Li et al., "Analysis and Design of Virtual Synchronous Machine based STATCOM Controller," *2014 IEEE 15th Workshop on Control and Modeling for Power Electronics (COMPEL)*, Santander, Spain, pp. 1-6, 2024. [CrossRef] [Google Scholar] [Publisher Link]

[7] Nitin Kumar, Omkar N. Buwa, and Mohan P. Thakre, "Virtual Synchronous Machine based PV-STATCOM Controller," *2020 IEEE First International Conference on Smart Technologies for Power, Energy and Control (STPEC)*, Nagpur, India, pp. 1-6, 2020. [CrossRef] [Google Scholar] [Publisher Link]

[8] Ghias Farivar et al., "Low-Capacitance Cascaded H-Bridge Multilevel StatCom," *IEEE Transactions on Power Electronics*, vol. 32, no. 3, pp. 1744-1754, 2017. [CrossRef] [Google Scholar] [Publisher Link]

[9] Ch. Lokeshwar Reddy et al., "A Five Level Cascaded H-Bridge Multilevel STATCOM," *2015 IEEE Asia Pacific Conference on Postgraduate Research in Microelectronics and Electronics (PrimeAsia)*, Hyderabad, India, pp. 36-41, 2015. [CrossRef] [Google Scholar] [Publisher Link]

[10] Akhil Gupta, "Power Quality Evaluation of Photovoltaic Grid Interfaced Cascaded H-Bridge Nine-Level Multilevel Inverter Systems using D-STATCOM and UPQC," *Energy*, vol. 238, 2022. [CrossRef] [Google Scholar] [Publisher Link]

[11] Anil Bharadwaj Chivukula, and Suman Maiti, "Analysis and Control of Modular Multilevel Converter-Based E-STATCOM to Integrate Large Wind Farms with the Grid," *IET Generation, Transmission & Distribution*, vol. 13, no. 20, pp. 4604-4616, 2019. [CrossRef] [Google Scholar] [Publisher Link]

[12] J. Venkataramanaiah, Y. Suresh, and Anup Kumar Panda, "A Review on Symmetric, Asymmetric, Hybrid and Single DC Sources based Multilevel Inverter Topologies," *Renewable and Sustainable Energy Reviews*, vol. 76, pp. 788-812, 2017. [CrossRef] [Google Scholar] [Publisher Link]

[13] Zhixing He et al., "Reactive Power Strategy of Cascaded Delta-Connected STATCOM under Asymmetrical Voltage Conditions," *IEEE Journal of Emerging and Selected Topics in Power Electronics*, vol. 5, no. 2, pp. 784-795, 2017. [CrossRef] [Google Scholar] [Publisher Link]

[14] Ali Zafari, and Mostafa Jazaeri, "STATCOM Systems in Distribution and Transmission System Applications: A Review of Power-Stage Topologies and Control Methods," *International Transactions on Electrical Energy Systems*, vol. 23, no. 2, pp. 323-346, 2015. [CrossRef] [Google Scholar] [Publisher Link]

[15] Heng Wu et al., "Small-Signal Modeling and Parameters Design for Virtual Synchronous Generators," *IEEE Transactions on Industrial Electronics*, vol. 63, no. 7, pp. 4292-4303, 2016. [CrossRef] [Google Scholar] [Publisher Link]

[16] Yuan Jian, and Yang Wei, "Precise Power Allocation Control Strategy for Multiple Virtual Synchronizers in Standalone Microgrids," *Power System Protection and Control*, vol. 47, no. 4, pp. 35-42 2019. [CrossRef] [Google Scholar] [Publisher Link]

[17] Cheng Zixia, Yu Yang, and Chai Xuzheng, "Research on Operation Control of Photovoltaic Storage VSG Based on Collaborative Adaptive Control," *Power System Protection and Control*, vol. 48, no. 24, pp. 79-85, 2020. [CrossRef] [Google Scholar] [Publisher Link]

[18] Yan Xiangwu, Cui Sen, and Jia Jiaoxin, "VSG Power Decoupling Strategy based on Virtual Steady-State Synchronous Negative Impedance," *Power System Protection and Control*, vol. 48, no. 18, pp. 102-113, 2020. [CrossRef] [Google Scholar] [Publisher Link]

[19] Miguel Castilla et al., "Coordinated Reactive Power Control for Static Synchronous Compensators under Unbalanced Voltage Sags," *2012 IEEE International Symposium on Industrial Electronics*, Hangzhou, China, pp. 987-992, 2012. [CrossRef] [Google Scholar] [Publisher Link]